JOURNAL OF GEOPHYSICAL RESEARCH, VOL. 102, NO. B9, PAGES 20,343–20,353, SEPTEMBER 10, 1997

Spatial distribution of snow in western Dronning Maud Land, East Antarctica, mapped by a ground-based snow radar

Cecilia Richardson,[1] Eldar Aarholt,[2] Svein-Erik Hamran,[3]
Per Holmlund,[1] and Elisabeth Isaksson[4]

Abstract. During the austral summer 1993/1994, the spatial distribution of snow was mapped by a ground-based snow radar (800–2300 MHz) in western Dronning Maud Land, East Antarctica. Snow radar soundings were performed along continuous profiles extending from the ice shelf up to the polar plateau, a total distance of 1040 km. The high-resolution radar registrations revealed subsurface layering in the uppermost 12 m of the snowpack. The travel time record was translated into snow accumulation expressed in water equivalents, based on an empirical relationship between wave speed and firn density. A good knowledge on snow density variations with depth is essential for the variability studies. Generally, the snow layering was well developed in the coastal area and less well developed on the polar plateau. High spatial variability in snow accumulation was observed on a regional as well as on a local scale. The variability was very high in areas with large surface slopes, such as the grounding zone and around nunataks. The highest variability was recorded in the nunatak area, where the standard deviation reached 59% of the spatial average accumulation. On the smooth high-altitude plateau, variations in accumulation were less pronounced. However, here the standard deviation exceeded 22% of the average accumulation rate. Provided that the snow radar soundings are supported by dating of reference horizons along the travel route, this is a good method to obtain the accumulation rate and pattern for large areas with a high spatial resolution.

1. Introduction

Accurate information on snow accumulation is of fundamental importance in glacier mass balance studies. The main traditional surveying method consists of repeated stake measurements, stratigraphic studies in snow pits, and more recently also chemical and physical analysis of firn cores. The accumulation pattern of the investigated areas is estimated from such point measurements. These techniques provide little information about the actual variability in snow accumulation. The principal uncertainty of the accumulation pattern constructed from point data is that the snow accumulation varies locally over the surface. The Antarctic ice sheet is huge, covering an area of 13.5×10^6 km^2. The available information on snow accumulation is sparse and concentrated to the most accessible regions close to the coasts. Important accumulation data from the interior of Antarctica have been reported in previous studies [cf. *Gow et al.*, 1972; *Young et al.*, 1982; *Giovinetto and Bull*, 1987; *Takahashi et al.*, 1994; *Mosley-Thompson et al.*, 1995]. However, the existing field data on snow accumulation are insufficient for reliable estimates of the total accumulation. In ice flow models, accumulation distribution is often described by simplified relationships between snow accumulation and parameters such as air temperature, surface elevation, latitude, and distance from open sea. Both mass balance studies and ice sheet modeling require improved understanding of Antarctic surface accumulation.

Stratified polar firn with layers of differing density has been reported and discussed in several Antarctic studies [cf. *Alley*, 1988; *Palais et al.*, 1982; *Rott et al.*, 1993; *West et al.*, 1996]. Combined stratigraphic analyses of visible layering of firn, firn density, and oxygen isotopes have been used to derive accumulation rates [*Goodwin*, 1991]. In stratigraphic firn core analysis, electrical conductivity of ice has proven to be very useful [cf. *Moore et al.*, 1992; *Taylor et al.*, 1992]. Ground-based radar systems have been used for studies of snow stratigraphy and estimations of water equivalence [cf. *Ellerbruch and Boyne*, 1980; *Annan et al.*, 1994; *Zabel et al.*, 1995; *Kohler et al.*, 1997]. Internal layers at greater depths within ice have often been observed in radar surveys of polar ice sheets [cf. *Harrison*, 1973; *Gudmandsen*, 1975; *Jacobel et al.*, 1993]. These reflecting horizons have been attributed to various features such as layers of differing density [cf. *Paren and Robin*, 1975; *Clough*, 1977] and layers of acidity due to volcanic eruptions [*Hammer*, 1980; *Millar*, 1981] and to changes in ice crystal fabric [*Fujita and Mae*, 1993; *Fujita et al.*, 1993; *Fujita and Mae*, 1994].

In this study we have used a ground-based snow radar to map variations in snow layer thickness in the upper 12 m of the snow pack in Dronning Maud Land, Antarctica. *Jonsson* [1988] and *Holmlund and Näslund* [1994] have described the physical geography in the study area. Spatial and temporal variations in accumulation and temperature within the study area have been investigated by firn core analysis and stake measurements [*Isaksson*, 1992; *Isaksson and Karlén*, 1994a, b; *Isaksson et al.*, 1996]. Radar surveys have been made along profiles and in grid nets associated with firn coring sites during the Swedish Antarctic Research Programme (SWEDARP) expeditions in 1991/

[1]Department of Physical Geography, Stockholm University, Stockholm, Sweden.
[2]Teleplan AS–Norconsult Telematics, Lysaker, Norway.
[3]Forsvarets forskningsinstitutt, Avdeling for elektronikk, Kjeller, Norway.
[4]Norsk Polarinstitutt, Oslo, Norway.

Paper number 97JB01441.
0148-0227/97/97JB-01441$09.00

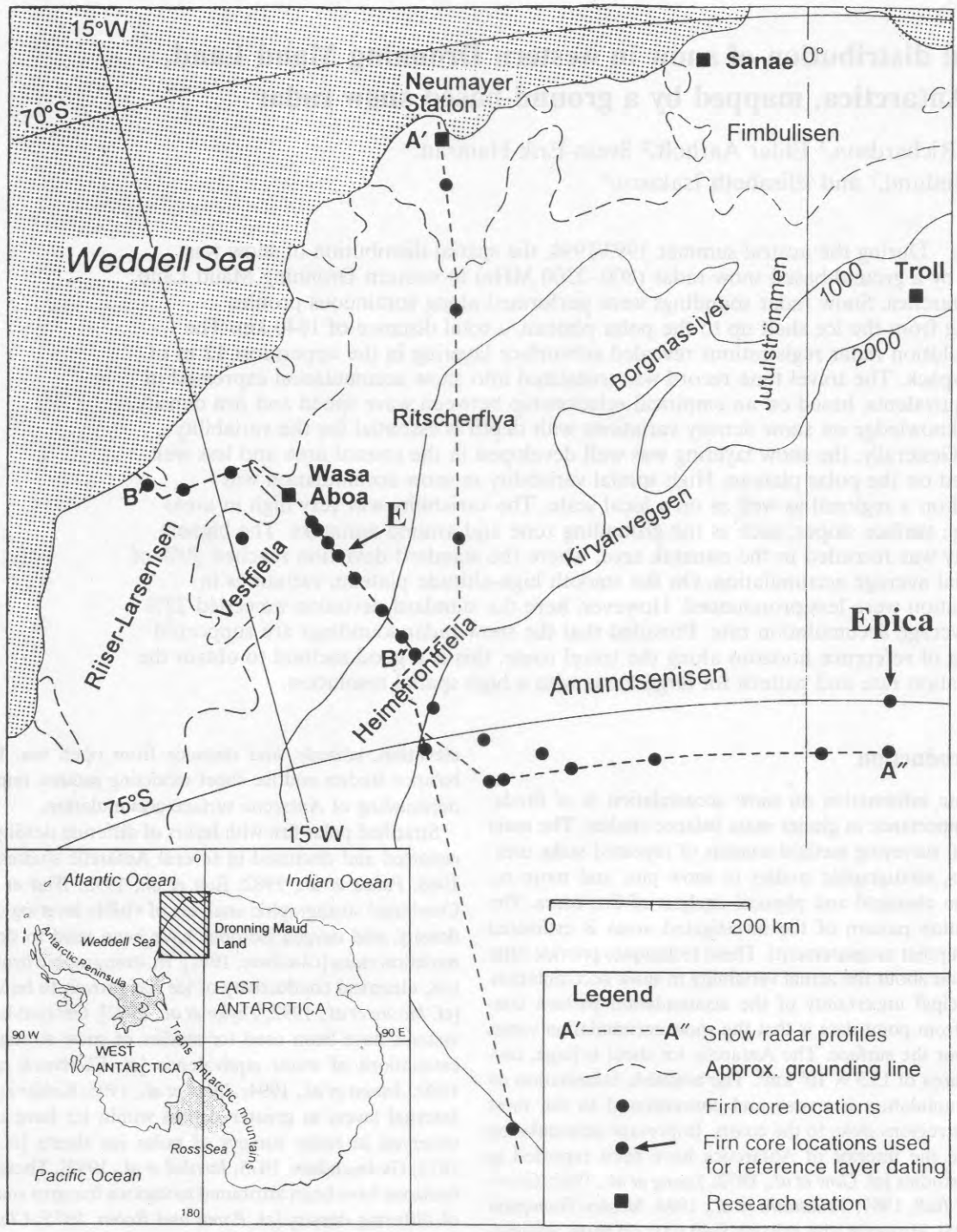

Figure 1. Location map of the study area in Dronning Maud Land. The escarpment zone bordering the polar plateau follows approximately the 2000 m above sea level (asl) contour line. Snow radar profiles and firn coring locations are indicated. Note the two reference firn cores named Epica and E.

1992 and 1993/1994. We report results from the 1993/1994 surveys, including a 1040 km long continuous radar profile revealing variations in snow accumulation from the ice shelf to the polar plateau (A′–A″, see Figure 1). The project is part of the International Trans-Antarctic Scientific Expedition (ITASE).

2. Equipment

The radio-echo sounder, which is based on a Hewlett & Packard Network Analyser (HP8753C), has been developed by the Environmental Surveillance Technology Programme in Norway [*Hamran and Aarholt*, 1993; *Hamran et al.*, 1995]. The

Figure 2. The snow radar antennae (indicated by arrows) were mounted on a steel frame on an all terrain carrier. The radio-echo sounder was installed inside the vehicle.

snow radar has previously been used in studies of the accumulation pattern on Swedish mountain glaciers in combination with manual probing [*Holmlund and Richardson*, 1995; *Holmlund*, 1996]. The radar is a continuous-wave step-frequency radar, transmitting a sequence of 201 frequencies evenly distributed over an adjustable bandwidth with a maximum range of 0.1–3.0 GHz. The antennae used were of pyramidal log-periodic type (AEL APN-106AA) specified for 400–3000 MHz. The centre frequency used was 1550 MHz, and the bandwidth was set to 1500 MHz. Processing of raw data involves analysis of frequency, amplitude, and phase by means of inverse fast Fourier transformation (IFFT). The IFFT analysis translates the received amplitude and phase of recorded reflections into range profile dB values and determines the travel time record.

The radar was installed in an all terrain carrier, Hägglund BV 206D6, with the transmitting and receiving antennae mounted with 1 m separation externally on the chassis (Figure 2). The antenna height above the snow surface was typically 0.4 m depending on snow conditions. In areas with large sastrugis the antennae were slightly raised. The time interval between each recorded sample was 2 s, corresponding to a horizontal distance of about 5 m between adjacent sounding points. The radar registrations were positioned by Global Positioning System (GPS) registrations (GPS Trimble Navigator) every 5 km with a horizontal accuracy of ±200 m.

3. Methods

The dielectric constant in snow and firn is affected by various physical and chemical parameters such as liquid water content, snow density, crystal fabric, conductivity, concentration, and composition of ions and microparticles. In Antarctic snow, several of these parameters have a seasonal variation which constitutes the base for stratigraphic studies. In radar studies the different physical and chemical properties of subsurface layers produce different reflection intensities due to variations of the dielectric constant. The radar registrations display the dB levels of recorded reflections (Figures 3 and 4), and some

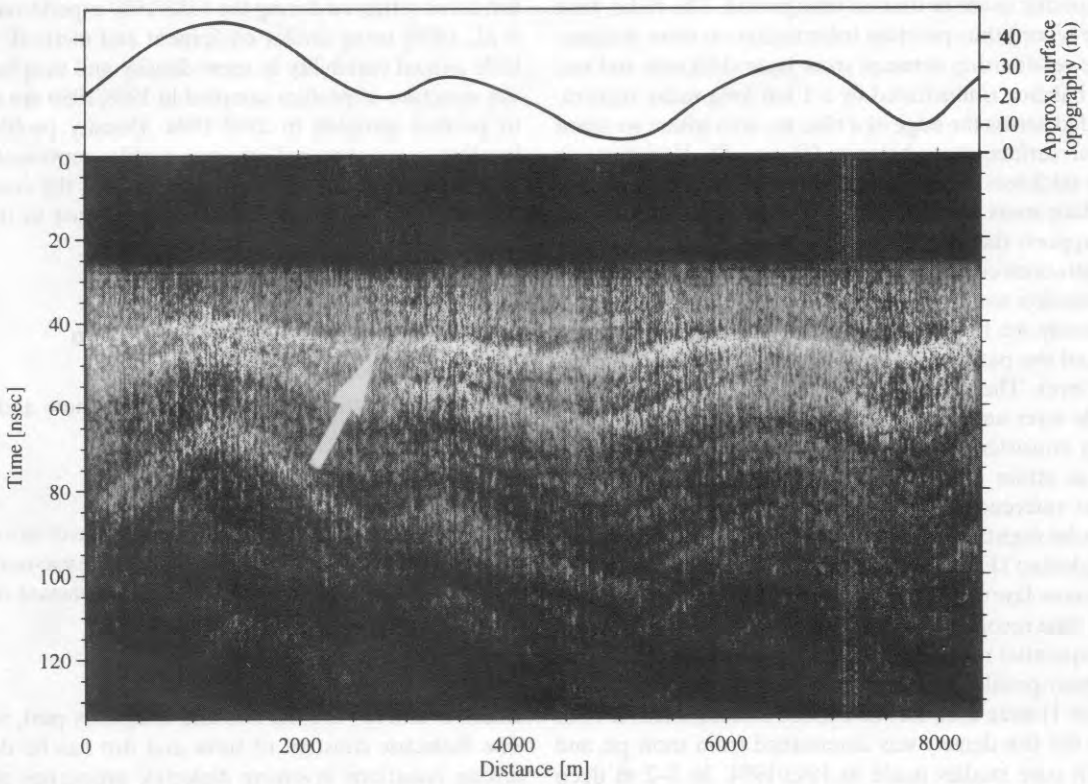

Figure 3. Snow radar registration from the coastal area recorded about 150 km from the coast. Several snow layers are clearly seen in the registration. The arrow indicates the reference layer used in the calculation. The maximum travel time corresponds to a snow depth of about 11.5 m.

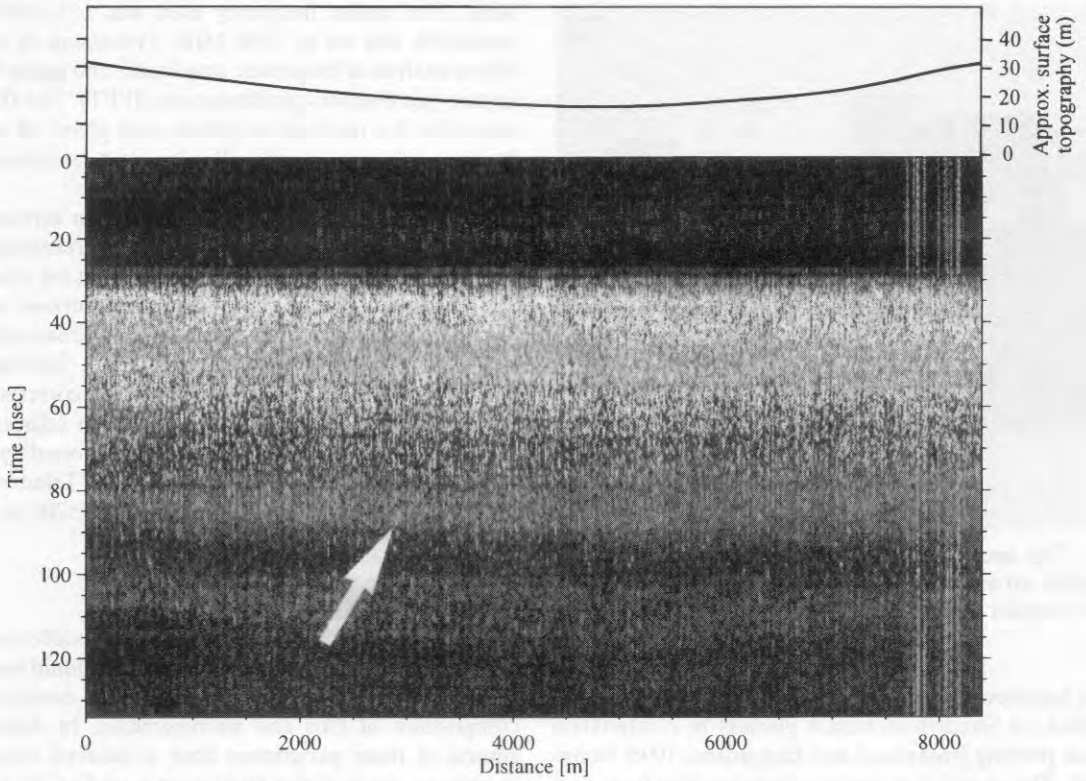

Figure 4. Snow radar registration from the polar plateau. Note that only a few layers are easy to distinguish and the reference layer is indicated. The maximum travel time corresponds to a snow depth of about 12 m.

snow layers appear more distinct than others. Our analysis is based on the assumption that a selected reference layer represents a specific event or limited time period. The radar wave travel time record thus provides information on snow accumulation. The relationship between snow layer thickness and surface mass balance is illustrated by a 1 km long radar registration recorded across the edge of a blue ice area where we know the general surface mass balance (Figure 5). Variations in snow layer thickness along the profile qualitatively describe the actual surface mass balance situation. The radar registration strongly supports the assumption that layers observed in snow radar registrations constitute time horizons which may be used for accumulation studies.

In the study we have used both the snow layer reflection intensity and the pattern of the layer sequence to identify the reference layer. The relation between the reflection intensity of a specific layer and that of other layers in the sequence was not always consistent in different locations, which made it necessary to utilize the layer sequence pattern for identification of the reference layer. The large differences observed between radar registrations recorded in the coastal area and on the polar plateau (Figures 3 and 4) made it impossible to use the same snow layer as reference horizon in the two regions. The travel time recorded for the reference layer was registered through sequential radar registrations by digitizing.

Firn density profiles obtained from 26 sites within the study area (Figure 1) were used for wave speed calculations. At 14 of these sites the firn density was determined from snow pit and shallow firn core studies made in 1993/1994. In 1–2 m deep snow pits, the firn was sampled in 0.03 m sections. Ten to twenty meter long firn cores were drilled with a Polar Ice Coring Office (PICO) light weight corer with a 3 inch barrel, and firn density was determined for core sections of 0.1–0.6 m. The remaining 12 density profiles were derived from shallow firn cores retrieved during the 1988/1989 expedition [*Holmlund et al.*, 1989] using similar equipment and method. We assume little annual variability in snow density and thus that the density structure of profiles sampled in 1988/1989 are comparable to profiles sampled in 1993/1994. Density profiles from 26 localities were averaged into two profiles representing characteristic densities for the polar plateau and the coastal region, respectively, based on the analysis presented in the next section.

4. Wave Speed in the Upper 15 m of the Firn Column

Electromagnetic wave speed through snow and firn is described by

$$c = c_0/\sqrt{|\varepsilon|} \tag{1}$$

where c is the speed of electromagnetic waves in snow/firn, c_0 is the speed of electromagnetic waves in a vacuum (0.2998×10^9 m/s), and ε is the complex dielectric constant of snow/firn, expressed by

$$\varepsilon = \varepsilon' - i\varepsilon'' \tag{2}$$

where ε' and $i\varepsilon''$ are the real and imaginary part, respectively. The dielectric constant of snow and firn can be described by mixing equations involving dielectric properties of the three weighted constituents: air, ice, and liquid water (if present). There are numerous models predicting the dielectric behavior of snow, with the more refined mixing formulae also taking

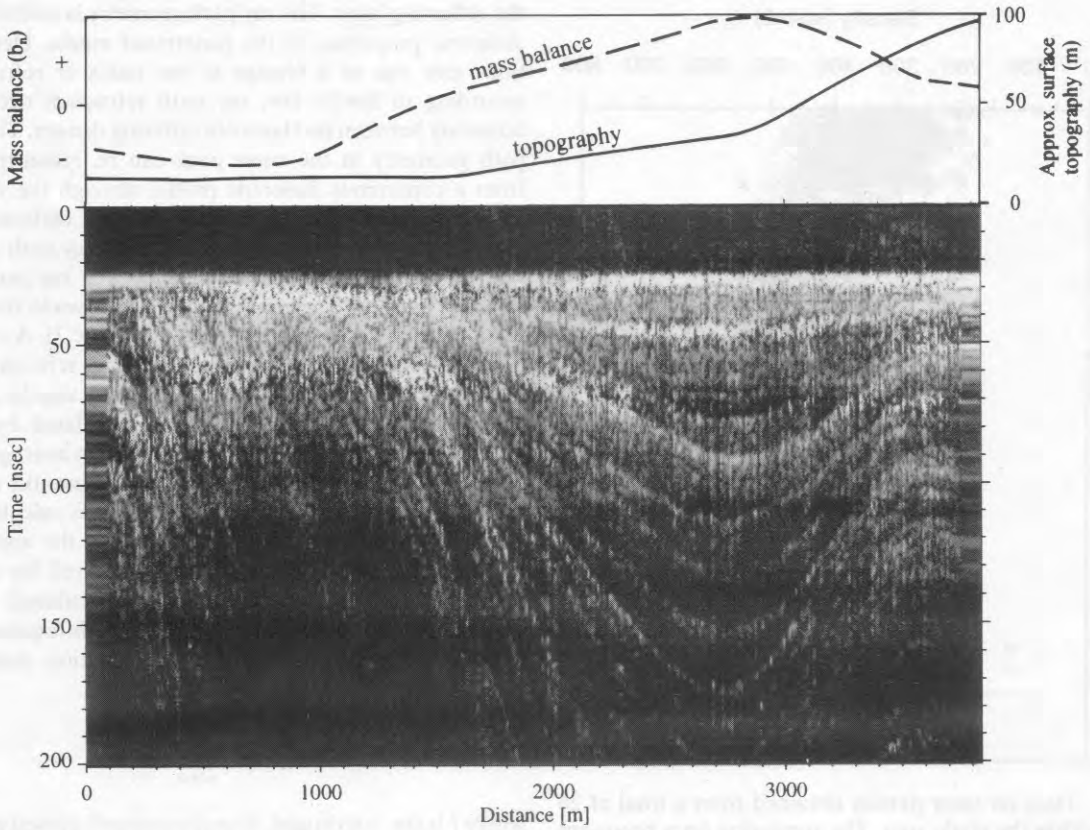

Figure 5. Snow radar registration recorded across the margin of a blue ice area. The profile follows the general ice flow direction within the area (from right to left). The surface mass balance is negative in the blue ice area, with steeply inclined layers that are cut off at the surface (0–300 m). The profile continues up a snow-covered slope with initially increasing accumulation (400–800 m). Approaching the top of the hill, accumulation again decreases (800–1000 m). The variations in snow layer thickness perfectly follow known mass balance variations along the profile.

into account the microscopic structure of the snow [cf. *Sihvola et al.*, 1985; *Mäzler*, 1987]. However, laboratory experiments indicate that the complex dielectric constant is practically independent of the snow structure [*Tiuri et al.*, 1984].

In the absence of liquid water, $|i\varepsilon''| \ll |\varepsilon'|$, and thus the imaginary part of the dielectric constant is negligible. In Dronning Maud Land, surface ablation by melting rarely occurs [*Zwally and Fiegles*, 1994] so the snow and firn are considered dry, and hence

$$c = c_0/\sqrt{|\varepsilon'|}. \tag{3}$$

In experiments with dry snow of densities up to 500 kg/m^3, *Tiuri et al.* [1984] found that apart from the effects of fabric changes, the real part of the dielectric constant was almost solely dependent on the snow density. The density profiles we have used in this study reach 500 kg/m^3 at snow depths of about 5 m, but few laboratory experiments have been concerned with snow densities exceeding 500 kg/m^3. In situ surveys for determining the relationship between the dielectric constant of polar firn and firn density [*Kovacs et al.*, 1995] resulted in the empirical equation

$$\varepsilon' = (1 + 0.845\rho)^2 \tag{4}$$

where ρ represents the specific gravity, i.e., the density relative to density of water. Equation (4) is valid for snow, firn, and ice.

According to *Mäzler* [1987], scattering effects are negligible when the wavelength of the electromagnetic signal is sufficiently larger than the grain size of the snow. The radar surveys presented here were made at wavelengths between 0.12 and 0.37 m, making scattering effects negligible. Provided that the frequency is sufficiently larger than the relaxation frequency of ice and that the wavelength is sufficiently larger than the grain size of snow, the real part of the dielectric constant of snow, ε', is independent of radar frequency. These conditions are satisfied over a large frequency interval from about 10 MHz to 10 GHz [*Mäzler*, 1987].

Generally, firn density increases with increasing depth, and thus the density-depth profile will influence the wave speed/depth profile for propagation of electromagnetic waves. Furthermore, snow density may vary between different regions due to local meteorological conditions, for example, air temperature, wind activity, and solar radiation. The nature of the terrain in the study area justifies an initial division into two geographic regions: the high-altitude polar plateau and the lower coastal region. The Antarctic polar plateau is in places bordered by nunatak areas, causing a dramatic change in surface elevation. In the study area the polar plateau is bordered by an escarpment zone that approximately follows the 2000 m above sea level (asl) contour line (Figure 1). The difference in altitude between the plateau and the lower coastal areas is typically 500–1500 m. On the polar plateau the densification process of snow and firn is depressed by lower air temperatures

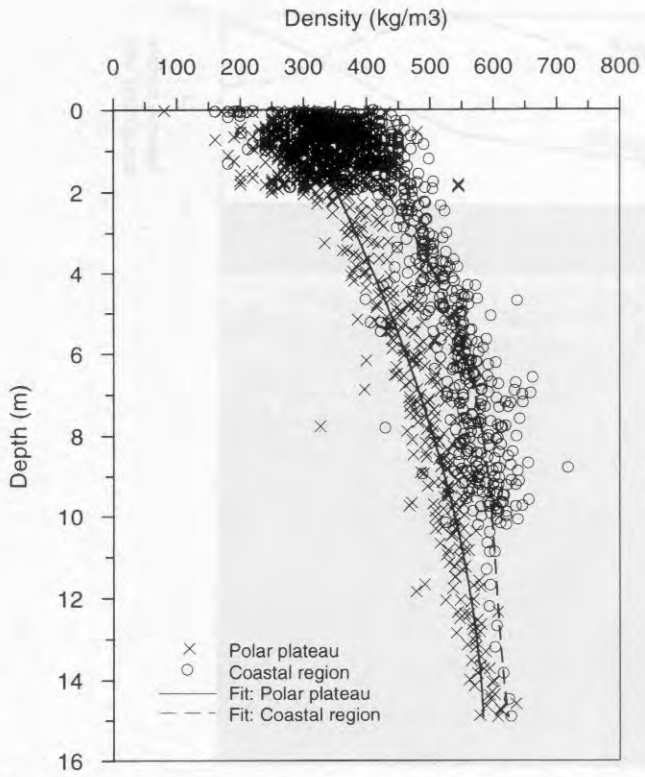

Figure 6. Data on snow density obtained from a total of 26 localities within the study area. The regression lines represent the average density profiles constructed for the polar plateau and the coastal region.

relative to the warmer coastal region. Moreover, the nunatak escarpment zone acts as a barrier for low-pressure weather systems common to the coastal area. For these reasons, the density profiles differ between the two regions (Figure 6), with higher densities in the coastal area and lower on the polar plateau. Further subdivision of the areas was not possible from comparisons of individual density profiles. The two density profiles representing an average of the density data available for each region were obtained by a regression analysis. The data sets were fitted by exponential and logarithmic functions and first- to fifth-degree polynomials. Third-degree polynomials describe the data sets well (Figure 6). The average functions representing the density profiles of the polar plateau (ρ_p) and the coastal region (ρ_c) measured in kilograms per cubic meter are

$$\rho_p = -0.144d_s^3 - 0.7168d_s^2 + 33.67d_s + 288.53 \quad (5)$$

$$R^2 = 0.78$$

and

$$\rho_c = 0.153d_s^3 - 5.3405d_s^2 + 66.062d_s + 342.32 \quad (6)$$

$$R^2 = 0.79,$$

where d_s is the snow depth in meters.

5. Vertical Reflection Depths and Water Equivalents

Recorded travel times represent wave propagation along the shortest time path from transmitting to receiving antennae via the reflecting layer. The ray path geometry is controlled by the dielectric properties of the penetrated media. Density variations give rise to a change in the index of refraction, and according to Snell's law, ray path refraction occurs at any boundary between two layers of differing density. The exact ray path geometry in the snow pack can be reconstructed only from a continuous dielectric profile through the vertical air-snow column. In absence of such detailed dielectric data we choose to apply a simplified model. The ray path is assumed vertical through the air. Subsequently, the ray path bends at the snow surface to follow a straight line down to the reflection point centred between the antennae (Figure 7). A relationship between recorded travel time and vertical reflection depth is then established. For selected reflection depths the corresponding nonvertical travel time is calculated by the wave speed obtained from (3) and (4). The 15 m average snow/firn column (equations (5) and (6)) is divided into 0.1 m sections, and for each section a mean wave speed is calculated as the average between velocities determined for the upper and the lower section limits. The travel time required for nonvertical passage through sequential sections is calculated, and subsequently, the total travel time (t_{tot}) in seconds required for wave passage single way to the selected reflection depths (d_r) is calculated by

$$t_{tot} = \sum_{i=0.0}^{d_r} l/c_i \quad (7)$$

where l is the nonvertical distance (meters) passed through the individual 0.1 m section and c_i is mean wave speed for sequen-

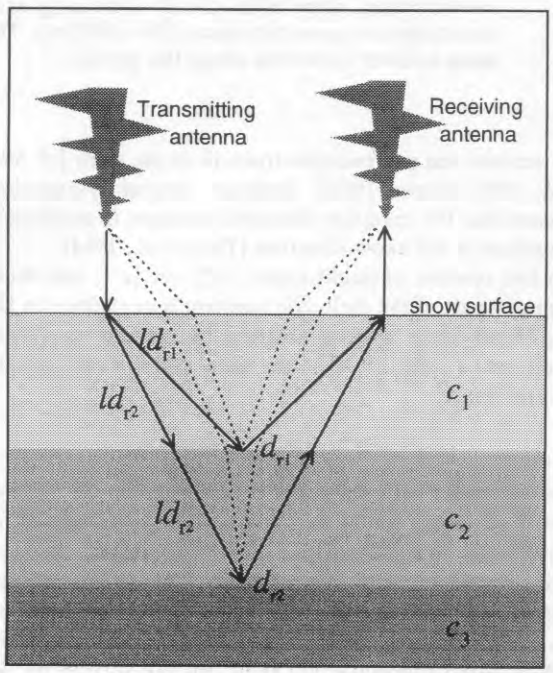

Figure 7. Cross section of a layered snow pack with two hypothetical reflection depths, d_{r1} and d_{r2}. The solid line represents the wave path geometry assumed in our model. The total travel time, t_{tot}, required for wave propagation through d_{r1} and d_{r2} is calculated from the mean wave speeds, c_1 and c_2, for the depth sections and the length of the travel distance, ld_{r1} and ld_{r2}, through each depth section. The dotted line schematically shows the real wave propagation geometry with refraction at layer boundaries.

tial sections (meters per second). The subscript i increases by steps of 0.1 from 0.0 to d_r. The relationship between total travel time and reflection depth is determined through numerical fitting (Figure 8), giving

$$d_p = -6.48387 \times 10^{-10} t_{tot}^6 + 1.49478 \times 10^{-7} t_{tot}^5 - 1.33925 \times 10^{-5} t_{tot}^4 + 0.000590125 t_{tot}^3 - 0.0136065 t_{tot}^2 + 0.376924 t_{tot} - 0.565216 \quad (8)$$

$$d_c = -5.12829 \times 10^{-10} t_{tot}^6 + 1.23204 \times 10^{-7} t_{tot}^5 - 1.154437 \times 10^{-5} t_{tot}^4 + 0.000534919 t_{tot}^3 - 0.0129802 t_{tot}^2 + 0.364842 t_{tot} - 0.555798 \quad (9)$$

where d_p and d_c refer to vertical reflection depth in meters on the polar plateau and in the coastal region, respectively, and t_{tot} denotes the recorded single-way travel time given in nanoseconds. After necessary travel time corrections for cabling and passage through air from antennae to snow surface, (8) and (9) are applied to the recorded travel times. Finally, the water equivalent of the snow overlying the reference horizon is calculated from the computed reflection depth and average cumulative density profiles resulting from (5) and (6). We have tested the error introduced in the model by neglecting Snell's law, and we found that errors are insignificant. The error decreases exponentially with increasing depth. For a snow depth of 0.6 m the deviation is less than 10% of the reflection depth, and for snow depths exceeding 2 m the deviation is less than 0.8%. The reference layers recorded in this study have an average snow depth of 2.6 m in the coastal area and 5.3 m on the polar plateau.

The layer sequence in the radar registrations may be dated by comparisons with dated firn cores. Unfortunately, the dating of the cores retrieved along the 1993/1994 radar sounded transects is still under processing. In order to make a provisional estimate of the age of the reference horizon, we have used data from two firn cores collected in the study area during 1991/1992. The two firn cores, called Epica and E (see Figure 1), were described and analyzed in detail for temporal accumulation and temperature variations by *Isaksson et al.* [1996]. Uncertainties are introduced by the fact that the firn cores were drilled 2 years prior to the radar soundings, and thus new features have been added to the stratigraphy that was recorded in the cores. The exact positioning of the coring sites poses additional problems. The Epica core was drilled at a location about 50 km north of the snow radar profile. The E core was not drilled along the snow radar profile A′–A″ that we present in this study but along the intersecting profile B′–B″ (see Figure 1). The E core chronology was first used to date the reference layer of profile B′–B.″ At the intersection point B″ the dated B′–B″ snow layer sequence was used to date the reference layer for the coastal part of the A′–A″ profile. Owing to this tentative dating, all values on accumulation rates given in this paper should be considered tentative.

As previously mentioned, different reference layers had to be used on the polar plateau and in the coastal region. On the polar plateau the reference layer was interpreted as representing a acidic horizon deposited in Antarctica during the years 1963–1965, caused by the 1963 volcanic eruption of Mount Agung [*Delmas et al.*, 1985]. Snow deposited above the reference horizon was thus assumed to represent 30 years of accumulation. In the coastal region where the accumulation rate is significantly higher, a younger reference layer was selected. In the coastal region the depth of the reference layer was interpreted to represent 6 years of snow accumulation.

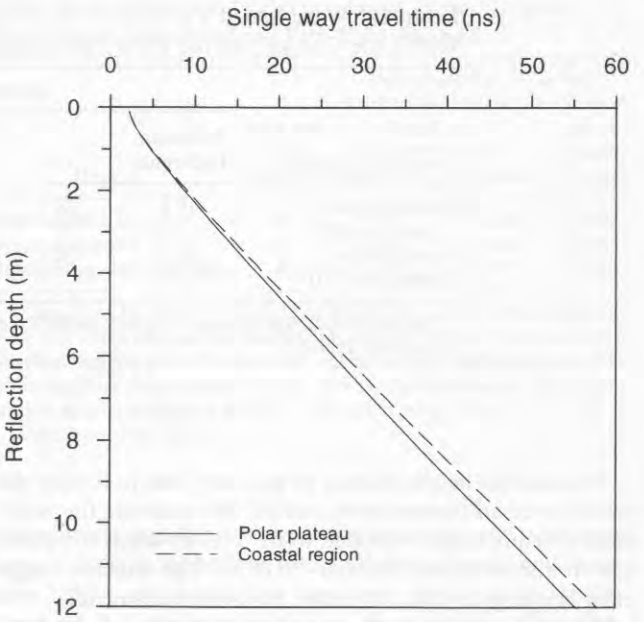

Figure 8. Relationships between recorded travel time and corresponding reflection depth for the polar plateau and the neighboring coastal region, valid for the antenna configuration described. Travel times were calculated for 34 selected reflection depths based on wave speed variations which are controlled by the density profiles in Figure 6.

6. Error Considerations

Uncertainties in the snow depth and water equivalent calculations originate from four main sources: (1) the instrument digitization capacity, (2) the spatial variability in snow density within the two the coastal region and the polar plateau, (3) the antenna height variations, and (4) the interpretation of the radar registrations.

The digitization error (source 1) is very small due to the long integration time used in this radar system (333 μs). For the frequencies used, the maximum digitization uncertainty is equivalent to a snow depth of 0.0004 m.

The error introduced by local snow density variations (source 2) within the coastal and the polar plateau regions has been tested. The wave propagation through the maximum and the minimum depth-density profiles measured in each region were ray traced in steps of 0.05 m from a depth of 0.1 to 8 m. The results were compared to an identical ray tracing through the average depth-density profile used for each region (equations (5) and (6)). The means of the difference between the lowest and the highest measured depth-density profile values and the average depth-density profile for the coastal region and the polar plateau were calculated (Table 1). The standard deviation and the wave velocity variation are also shown. The differences in wave velocity between the worst case depth-density profile values measured and that of the average depth-density profiles applied are of the order of 4–9% of the calculated snow depth values.

Table 1. Wave Speed Variations Due to Spatial Variations in the Depth-Density Profiles Within the Coastal and the Polar Plateau Regions

Geographic Region	Density Values, kg/m^3					Wave Speed Variation, %
	Minimum Difference	s.d.	Maximum Difference	s.d.	Density Range	
Coastal region (equation (6))	19.1	28.7	26.6	26.2	300–600	4–8
Polar plateau (equation (5))	16.7	28.1	39.2	39.6	300–600	4.5–9

The maximum and minimum density profiles measured were compared to the average profiles for each geographic region.

The antenna height (source 3) may vary due to driving the vehicle over an uneven snow surface. We estimate the maximum antenna height variation to be ±0.1 m which is equivalent to a snow depth of about ±0.08 m. The antenna height error is not systematic but rather has a noisy character.

The interpretation accuracy (source 4) is dependent on the range resolution of the radar system. The absolute range resolution in snow is of the order of 0.075 m, and by the use of interpolation methods in the IFFT the potential picking range resolution is improved to about 0.03 m. Here it must be noted that roughness at the medium interface will broaden the pulse. The reference layers interpreted in the radar registrations have a thickness which is typically equivalent to 0.1–0.3 m snow. The uncertainty in interpreting the correct position of the reflector is estimated to ±0.1 m snow.

Concluding the uncertainties related to snow depth and water equivalent estimations, the error originates mainly from spatial variations in the depth-density profiles. The uncertainty may reach ~4–9% of the snow depth values.

7. Results

The measured snow layer thickness shows large spatial variations over short distances (Figure 3). Over a distance of <5 km, the recorded snow layer thickness may vary by ±60–70% from the local average value. According to the radar registrations the spatial pattern of accumulation appears more or less constant from year to year, while substantial variations in absolute accumulation between years are indicated. Qualitative observations of local topography along the travel route indicate that thick snow layers are associated with depressions, and thin layers are associated with topographic highs. Snow layers generally appear more distinct close to the coast compared to those at higher elevations (see Figures 3 and 4). Nevertheless, in recordings from the polar plateau, at an altitude close to 3000 m asl, it is still possible to distinguish one or two layers. In areas with locally disturbed snow layering, lack of layering, or net mass loss due to wind erosion the reference layer is lost. Such areas are readily visible in the registrations. Crevasses

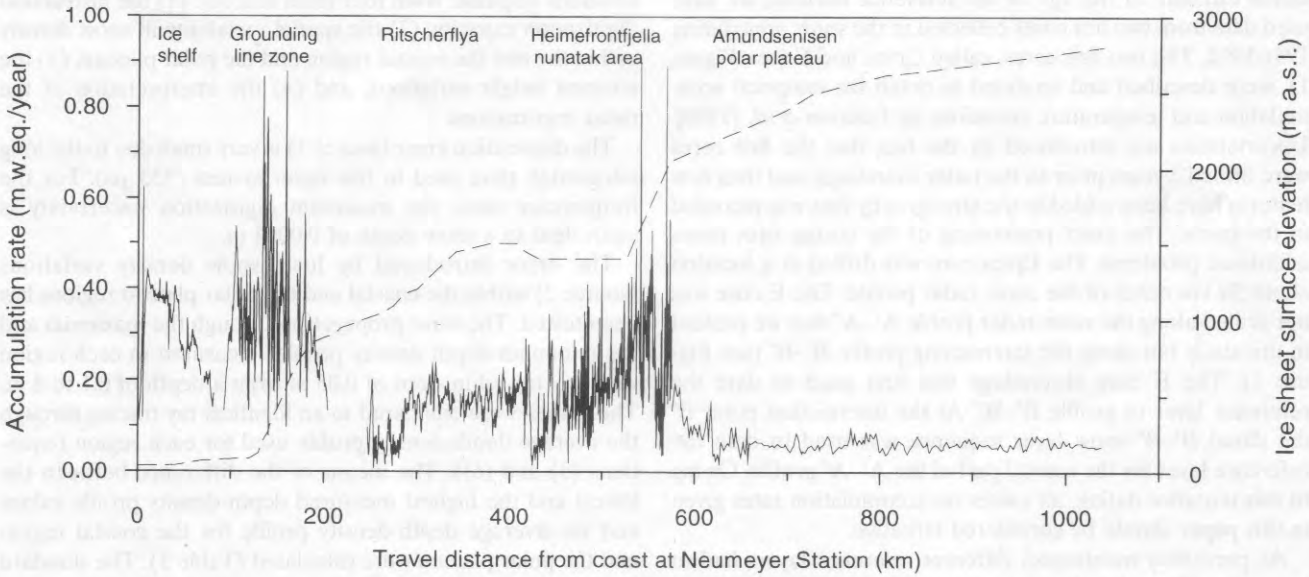

Figure 9. Variation of snow accumulation along the 1040 km long profile A′–A″ (Figure 1); surface elevation of the ice sheet is also shown. Note the very high spatial variability in snow accumulation. Absolute accumulation rates are tentative, based on preliminary dating of the reference layer. The curve represents an annual accumulation averaged over 30 years on the polar plateau and an accumulation averaged over 6 years in the coastal region.

buried beneath snow bridges are easy to distinguish in the radar registrations, appearing like empty space due to missing reflections.

The snow accumulation along the 1040 km long profile A′–A″ (Figure 1) is expressed in water equivalents (w. eq.) in Figure 9. The altitude data were obtained from barometer measurements in the coastal region and by differential GPS measurements on the polar plateau (unpublished data from the SWEDARP expeditions 1987/1988 and 1993/1994). On the ice shelf the snow accumulation decreases away from the coast line. The grounding zone is characterized by relatively high accumulation rates with great spatial variability. On the neighboring intermediate altitude area, Ritscherflya (Figure 1), the spatial variations are relatively small. Snow accumulation increases in the vicinity of the Heimefrontfjella mountain range, where local variations are considerable. On the Amundsenisen polar plateau the accumulation rate is relatively low and is associated with a comparatively even spatial distribution. Assuming that the identification and dating of reference layers are correct, average accumulation rates may be calculated for the specific regions. Statistics were calculated for the various accumulation environments (Table 2). The standard deviation is given in percent relative to the calculated average accumulation.

Ambiguities in the reference layer identification occurred due to locally disturbed layering, surface erosion, and temporary breaks in the continuous radar profile due to instrumental problems. Along the transect from the coast line to the nunatak area (Figure 9), ambiguities in the interpretation occurred at five locations, and in addition the reference layer was lost at two locations. In the nunatak area, ambiguities occurred 4 times, but no hiatus was recorded. On the polar plateau, there were two ambiguous interpretations.

8. Discussion

The large variations in accumulation rate shown in parts of Figure 9 reveal that there is a need for improved information on the spatial distribution of snow in addition to single point measurements. Variations in snow layer thickness were observed in association with topographic features, which suggest that wind redistribution have a major influence on the local accumulation pattern. This relation has also been recognized in several previous studies, such as *Black and Budd* [1964] and *Gow and Rowland* [1965]. The considerable spatial variability in snow accumulation observed indicates that the accumulation pattern is complex and that broad-scale Antarctic snow accumulation is difficult to describe by parameterization of air temperature, surface elevation, latitude, or distance from open water. This is in agreement with a study by *Fortuin and Oerlemans* [1990], who found that they were able to make reliable parameterizations only for the ice sheet interior. Our study indicates that a division into typical accumulation regions, such as in Table 2, is necessary to describe the accumulation pattern in the noncentral parts of the Antarctic ice sheet. On the ice shelf the accumulation rate shows a decreasing trend with increasing travel distance from the coast (Figure 9). This suggests a correlation between the accumulation rate and the distance from sea and/or the surface elevation. The decreasing trend explains part of the standard deviation which is relatively low, only 30% of the spatial average. Regions characterized by comparatively steep surface slopes, such as the grounding zone and the nunatak area, are associated with the highest recorded spatial variability in accumulation (Figure 9). Here the standard deviation amounts to 44% and 59%, respectively, of the aerial accumulation rate. In the nunatak area, parts of the variability may be explained by lee side accumulation and erosion effects due to wind channeling nearby individual nunataks. In the intermediate altitude area Ritscherflya and on the polar plateau, which both are characterized by a relatively flat topography, the standard deviation still reaches 33% and 37%, respectively, of the spatial average accumulation.

The observations of a generally static accumulation pattern from year to year combined with large interannual variations in absolute accumulation values are consistent with results from stake measurements within the study area [*Isaksson and Karlén*, 1994a]. The tentative accumulation rates obtained by radar have been compared with results by H. Moser (internal report 1990), who derived accumulation rates by oxygen isotope analysis of firn cores retrieved along the same profile as the radar soundings (Table 3). The firn core data set represent the years 1970–1986. The accumulation rates obtained by radar agree well with the firn core data. For the ice shelf and the grounding zone, the radar data are somewhat higher but still within the range of values obtained by the firn core study. For the part of Ritscherflya that is represented by both data sets (247–280 km from the coast) the accumulation values are similar. However, since the radar gives a spatial average value, accumulation surveys by snow radar are not expected to yield accumulation rates identical to data obtained from single point measurements. In this comparison it is also important to keep in mind that the accumulation data obtained from the two methods represent different time periods and that the radar

Table 2. Accumulation Rates Calculated for Typical Accumulation Environments

Accumulation Environment	Altitude, m asl	Mean Accumulation Rate, m w. eq.	s.d., %	Travel Distance From Coast, km
Ekströmsisen ice shelf	30–75	0.307	30	0–81
Grounding zone	75–1000	0.330	44	92–203
Ritscherflya	1000–1500	0.136	33	247–410
Heimefrontfjella nunatak area	1400–2050	0.200	59	410–575
Amunsenisen polar plateau	2200–2800	0.061	22	620–1038

Accumulation rates should be considered tentative. The travel distances given refer to Figure 9. Water equivalent, w. eq.

Table 3. Comparison of Accumulation Rates Obtained From Radar Soundings and Firn Core Analysis

Region	Number of Firn Cores*	Accumulation, m w. eq. Firn Core* Minimum	Firn Core* Maximum	Snow Radar Mean†
Ekströmsisen ice shelf	5	0.195	0.333	0.307
Grounding zone	7	0.205	0.364	0.330
Ritscherflya, 247–280 km	2	0.070	0.071	0.067

*Data from H. Moser (Institute of Hydrology, GSF-Forschungszentrum fuer Umwelt und Gesundheit Muenchen, Neuherberg, Germay, Untersuchungen zur akkumulation auf dem Filchner/Ronne-und Ekström-Shelfeis unter andwendung von isotopenmetoden mit ergänzenden stratigraphischen studien, internal report, Table 7.5, 1990).

†Data from this study.

data are based on a tentative dating. The accumulation rate obtained by radar on the polar plateau was 0.061 m w. eq. This is in agreement with *Giovinetto et al.* [1990], who used an accumulation rate of 0.05–0.10 m w. eq. for this area.

The difference in layer distinctness and number of visible layers between coastal areas and the polar plateau is probably due to several factors. Radar reflections are generated by differing dielectric constants. The firn density is very important for the dielectric constant [cf. *Tiuri et al.*, 1984; *Kovacs et al.*, 1995]. The strong layer reflections in the coastal area may be related to layers of high density developed as surface crusts during summer. Another important factor is the ionic content of the snow. It is known that the concentration and composition of ions not only have seasonal variation but also pronounced spatial variation [*Mulvaney and Wolff*, 1994]. Sea-salt ions, chosen as a simple example, are most abundant in the coastal area and decrease with altitude and distance from open sea. The spatial variations in ionic content are not well understood, but they may explain parts of the observed differences between the radar registrations.

The correctness of the reference layer dating controls the accuracy of the absolute accumulation rates obtained from snow radar soundings. In the study area the identification of the reference layer was most reliable at high altitudes, because there were only one or two easily distinguishable horizons. Greater interpretation problems arose in zones of low accumulation in coastal areas and in areas with net ablation or disturbed layering. In such problematic areas the risk that the reference layer may be mixed with neighboring layers can only be avoided by recurrent correlation to dated firn cores. Unfortunately, many dating methods available for firn cores are based on stratigraphy, and thus they are unable to provide an unambiguous chronology, e.g., annual layers may be missing because of wind erosion. It is preferable to use absolute dating methods such as tracing volcanic horizons or bomb layers. Frequent firn coring along the travel route is a good way to ensure a proper dating of the reference layer.

Determination of the spatial variability in accumulation is not dependent on dating of a reference layer. Every radar registration may be analyzed separately with respect to the accumulation variability, and all data available for a specified area may be put together. As long as there are no ambiguities in the interpretation of the radar registrations, the result represents a relative value of the spatial variability. At firn core sites, snow radar soundings performed in detailed grid nets are useful to evaluate how well accumulation data obtained from the cores represent the actual accumulation rate. Furthermore, areas with disturbed layering may be identified by snow radar soundings, information that is of utmost importance when selecting suitable firn coring sites. The surveys presented in this paper were performed within the context of the ITASE programme aiming at obtaining high-resolution data on climate, atmosphere, and surface conditions over the Antarctic ice sheet for the last 100–200 years. The snow radar method proved very useful for retrieving surface accumulation data within the ITASE and similar projects. Snow radar soundings also have a potential to provide ground truthing on microwave data needed in various satellite-based remote sensing techniques.

9. Conclusions

Significant regional spatial variations in accumulation rate, with high local variability, have been measured by radar along a 1040 km long continuous profile. Generally, the layering in the snow pack was well developed in the coastal region and less well developed on the polar plateau.

The accumulation pattern in western Dronning Maud Land appears complex and thus difficult to describe by simple relationships to various physical parameters. Both the regional and the local variability in snow accumulation are important. It seems useful to divide the study area into typical regions and to analyze the accumulation characteristics separately for each region. The spatial variability in accumulation rate in the study area was expressed as the standard deviation in percent of the aerial average accumulation rate for the region. On the Ekströmsisen ice shelf the accumulation decreased with increasing distance from sea and increasing surface elevation. The standard deviation was 30% of the aerial average accumulation rate. The highest spatial variability was recorded in areas with a pronounced surface slope. The standard deviation was 44% in the grounding zone and 59% of the aerial average accumulation in the Heimefrontfjella nunatak area. In areas with relatively flat surface topography, the standard deviation was less, it was 33% in the intermediate altitude area Ritscherflya and 22% on the Amundsenisen polar plateau.

Ground-based snow radar soundings provide an excellent method to map spatial variability in snow accumulation. Studies of variability must be supported by a good knowledge of snow density variations with depth. To obtain reliable values of absolute accumulation rates from radar soundings, accurate dating of the snow column is required. The method to determine snow accumulation from radar travel time records outlined in this paper yields accumulation rates that agree with results from firn core analysis. The accumulation data obtained give very detailed information on local variability, as the distance between adjacent radar soundings is of the order of a few meters. This type of information can be very important when assessing the spatial variability of accumulation data obtained from point measurements such as firn cores. Snow radar soundings are useful in accumulation studies covering large areas, and they are appropriate for surveys in the Antarctic coastal regions as well as on the polar plateau.

Acknowledgments. The project was financed by the Swedish Natural Science Research Council (NFR), the Department of Physical Geography at Stockholm University, the Wallenberg Foundation and OK's Environmental Foundation. We are very grateful to J.-O. Näslund and P. Jansson, Stockholm University; E. Nyfors, Multi-fluid Int.; and J. Lundstedt, KTH, for stimulating discussions and valuable comments on the manuscript. We would also like to thank S. Fujita, R. W. Jacobel, and an anonymous referee for their important and helpful comments. The language was kindly improved by J. Boygle. Many thanks are due to Hewlett-Packard and IBM, who lent us equipment in a most generous way. Thanks also to Geotronics, NOAB, and Verbatim for support. The logistics were provided by the Swedish Polar Research Secretariat, and finally, we would like to acknowledge the members of the 1991/1992 and 1993/1994 field parties.

References

Alley, R. B., Concerning the deposition and diagenesis of strata in polar firn, *J. Glaciol.*, *34*(118), 283–290, 1988.

Annan, A. P., S. W. Cosway, and T. Sigurdsson, GPR for snow pack water content, paper presented at the Fifth International Conference on Ground Penetrating Radar, Waterloo Cent. for Groundwater Res., Waterloo, Ontario, Canada, June 12–16, 1994.

Black, H. P., and W. Budd, Accumulation in the region of Wilkes, Wilkes Land, Antarctica, *J. Glaciol.*, *5*(37), 3–15, 1964.

Clough, J. W., Radio-echo sounding: Reflection from internal layers in ice sheets, *J. Glaciol.*, *18*(78), 3–14, 1977.

Delmas, R., M. Legrand, A. J. Aristarain, and F. Zanolini, Volcanic deposits in Antarctic snow and ice, *J. Geophys. Res.*, *90*(D7), 12,901–12,920, 1985.

Ellerbruch, D. A., and H. S. Boyne, Snow stratigraphy and water equivalence measured with an active microwave system, *J. Glaciol.*, *26*(94), 225–233, 1980.

Fortuin, J. P. F., and J. Oerlemans, Parameterization of the annual surface temperature and mass balance of Antarctica, *Ann. Glaciol.*, *14*, 78–84, 1990.

Fujita, S., and S. Mae, Relation between ice-sheet internal radio-echo reflections and ice fabrics at Mizuho Station, Antarctica, *Ann. Glaciol.*, *17*, 269–275, 1993.

Fujita, S., and S. Mae, Causes and nature of ice-sheet radio-echo internal reflections estimated from the dielectric properties of ice, *Ann. Glaciol.*, *20*, 80–86, 1994.

Fujita, S., S. Mae, and T. Matsuoka, Dielectric anisotropy in ice Ih at 9,7 GHz, *Ann. Glaciol.*, *17*, 276–280, 1993.

Giovinetto, M. B., and C. Bull, Summary and analysis of surface balance compilations for Antarctica, 1960–85, *Rep. 1*, Byrd Polar Res. Cent., Ohio State Univ., Columbus, 1987.

Giovinetto, M. B., N. M. Waters, and C. R. Bentley, Dependence of Antarctic surface mass balance on temperature, elevation and distance to open ocean, *J. Geophys. Res.*, *95*(D4), 3517–3531, 1990.

Goodwin, I., Snow-accumulation variability from seasonal surface observations and firn-core stratigraphy, eastern Wilkes Land, Antarctica, *J. Glaciol.*, *37*(127), 383–387, 1991.

Gow, A. J., and R. Rowland, On the relationship of snow accumulation to surface topography at "Byrd Station," Antarctica, *J. Glaciol.*, *5*(42), 843–847, 1965.

Gow, A. J., F. Blander, G. Crozaz, and E. Picciotto, Snow accumulation at "Byrd" station, Antarctica, *J. Glaciol.*, *11*(61), 59–64, 1972.

Gudmandsen, P., Layer echoes in polar ice sheets, *J. Glaciol.*, *15*(73), 95–101, 1975.

Hammer, C. U., Acidity of polar ice cores in relation to absolute dating, past volcanism and radio-echoes, *J. Glaciol.*, *25*(93), 359–372, 1980.

Hamran, S.-E., and E. Aarholt, Glacier study using wavenumber domain synthetic aperture radar, *Radio Sci.*, *28*(4), 559–570, 1993.

Hamran, S.-E., D. T. Gjessing, J. Hjelmstad, and E. Aarholt, Ground penetration synthetic aperture radar: Dynamic range and modes of operation, *J. Appl. Geophys.*, *33*, 7–14, 1995.

Harrison, C. H., Radio echo soundings of horizontal layers in ice, *J. Glaciol.*, *12*(66), 383–397, 1973.

Holmlund, P., Radar measurements of annual snow accumulation rates, *Z. Gletscherk. Glazialgeol.*, *32*, 193–196, 1996.

Holmlund, P., and J.-O. Näslund, The glacially sculptured landscape in Dronning Maud Land, Antarctica, formed by wet-based mountain glaciation and not by the present ice sheet, *Boreas*, *23*, 139–148, 1994.

Holmlund, P. and C. Richardson, Radar measurements of annual snow accumulation rates on Swedish glaciers, in *Tarfala Research Station Annual Report 1993/94*, edited by P. Jansson, *Rep. STOU-NG 102*, pp. 42–43, Dep. of Phys. Geogr., Stockholm Univ., Stockholm, Sweden, 1995.

Holmlund, P., E. Isaksson, and W. Karlén, Massbalans, isrörelse och isdynamik: Preliminära resultat från fältsäsongen 1988/89 i Vestfjella och Heimefrontfjella, V. Dronning Maud Land, Antarktis, *Rep. STOU-NG 73*, 66 pp., Dep. of Phys. Geogr., Stockholm Univ., Stockholm, Sweden, 1989.

Isaksson, E., Spatial and temporal patterns in snow accumulation and oxygen isotopes, western Dronning Maud Land, Antarctica, *Rep. STOU-NG 87*, 86 pp., Dep. of Phys. Geogr., Stockholm Univ., Stockholm, Sweden, 1992.

Isaksson, E., and W. Karlén, Spatial and temporal patterns in snow accumulation and oxygen isotopes, Western Dronning Maud Land, Antarctica, *J. Glaciol.*, *40*(135), 399–409, 1994a.

Isaksson, E., and W. Karlén, High resolution climatic information obtained from short firn cores, Western Dronning Maud Land, Antarctica, *Clim. Change*, *26*, 421–434, 1994b.

Isaksson, E., W. Karlén, N. Gundestrup, P. Mayewski, S. Whitlow, and M. Twickler, A century of accumulation and temperature changes in Dronning Maud Land, Antarctica, *J. Geophys. Res.*, *101*(D3), 7085–7094, 1996.

Jacobel, R. W., A. M. Gades, D. L. Gottschling, S. M. Hodge, and D. L. Wright, Interpretation of radar-detected internal layer folding in West Antarctic ice streams, *J. Glaciol.*, *39*(133), 528–537, 1993.

Jonsson, S., Observations on physical geography and glacial history of the Vestfjella nunataks in western Dronning Maud Land, Antarctica, *Rep. STOU-NG 68*, 57 pp., Dep. of Phys. Geogr., Stockholm Univ., Stockholm, Sweden, 1988.

Kohler, J., J. Moore, M. Kennett, R. Engeset, and H. Elvehøy, Using ground-penetrating radar to image previous years' summer surfaces for mass balance measurements, *Ann. Glaciol.*, *24*, in press, 1997.

Kovacs, A., A. J. Gow, and R. M. Morey, The in-situ dielectric constant of polar firn revisited, *Cold Reg. Sci. Technol.*, *23*, 245–256, 1995.

Mäzler, C., Applications of the interaction of microwaves with the natural snow cover, *Remote Sens. Rev.*, *2*, 259–392, 1987.

Millar, D. H. M., Radio-echo layering in polar ice sheets and past volcanic activity, *Nature*, *292*(5822), 441–443, 1981.

Moore, J. C., E. W. Wolff, H. B. Clausen, and C. U. Hammer, The chemical basis for the electrical stratigraphy of ice, *J. Geophys. Res.*, *97*(B2), 1887–1896, 1992.

Mosley-Thompson, E., L. G. Thompson, J. F. Paskievitch, M. Pourchet, A. J. Gow, M. E. Davis, and J. Kleinman, Recent increase in south pole snow accumulation, *Ann. Glaciol.*, *21*, 131–138, 1995.

Mulvaney, R., and E. W. Wolff, Spatial variability of the major chemistry of the Antarctic ice sheet, *Ann. Glaciol.*, *20*, 440–447, 1994.

Palais, J. M., I. M. Whillans, and C. Bull, Snow stratigraphic studies at dome C, East Antarctica: An investigation of depositional and diagenetic processes, *Ann. Glaciol.*, *3*, 239–242, 1982.

Paren, J. G., and G. de Q. Robin, Internal reflections in polar ice sheets, *J. Glaciol.*, *14*(71), 251–259, 1975.

Rott, H., K. Sturm, and H. Miller, Active and passive microwave signatures from Antarctic firn by means of field measurements and satellite data, *Ann. Glaciol.*, *17*, 337–343, 1993.

Sihvola, A., E. Nyfors, and M. Tiuri, Mixing formulae and experimental results for the dielectric constant of snow, *J. Glaciol.*, *31*(108), 163–170, 1985.

Takahashi, S., Y. Ageta, Y. Fujii, and O. Watanabe, Surface mass balance in east Dronning Maud Land, Antarctica, observed by Japanese Antarctic research expeditions, *Ann. Glaciol.*, *20*, 242–248, 1994.

Taylor, K., R. Alley, J. Fiacco, P. Grootes, G. Lamorey, P. Mayewski, and M. J. Spencer, Ice-core dating and chemistry by direct current electrical conductivity, *J. Glaciol.*, *38*(130), 325–332, 1992.

Tiuri, M. E., A. H. Sihvola, E. G. Nyfors, and M. T. Hallikainen, The complex dielectric constant of snow at microwave frequencies, *IEE J. Oceanic Eng.*, *OE-9*(5), 377–382, 1984.

West, R. D., D. P. Winebrenner, L. Tsang, and H. Rott, Microwave emission from density stratified Antarctic firn at 6 cm wavelength, *J. Glaciol.*, *42*(140), 63–76, 1996.

Young, N. W., M. Pourchet, V. M. Kotlyakov, P. A. Korolev, and M. B. Dyugerov, Accumulation distribution in the IAGP area, Antarctica: 90°E–150°E, *Ann. Glaciol.*, *3*, 333–338, 1982.

Zabel, I. H. H., K. C. Jezek, P. A. Baggeroer, and S. P. Gogineni, Ground-based radar observations of snow stratigraphy and melt processes in the percolation facies of the Greenland ice sheet, *Ann. Glaciol.*, *21*, 40–44, 1995.

Zwally, H. J., and S. Fiegles, Extent and duration of Antarctic surface melting, *J. Glaciol.*, *40*(136), 463–476, 1994.

E. Aarholt, Teleplan AS–Norconsult Telematics, Fornebuveien 33-35, P.O. Box 69, N-1324 Lysaker, Norway.

S.-E. Hamran, Forsvarets forskningstitutt, Avdeling for elektronikk, Postboks 25, N-2007 Kjeller, Norway.

P. Holmlund and C. Richardson, Department of Physical Geography, Stockholm University, S-106 91 Stockholm, Sweden.

E. Isaksson, Norsk Polarinstitutt, Middlethuns gate 29, P.O. Box 5072 Majorstua, N-0301 Oslo, Norway.

(Received May 21, 1996; revised May 7, 1997;
accepted May 13, 1997.)